J. Nano- Electron. Phys.
3 (2011) No1, P. 1127-1136

© 2011 SumDU
(Sumy State University)

PACS numbers: 84.60.Jt, 61.43.Bn

SIMULATION AND OPTIMIZATION OF N-TYPE PERL SILICON SOLAR CELL STRUCTURE

William R. Taube, A. Kumar

[1] Central Electronics Engineering Research Institute,
Pilani, India
E-mail: williamtaube@gmail.com

Optimization of structure and process parameters of PERL (Passivated Emitter Rear Locally Diffused) silicon solar cell using SILVACO software package has been carried out. PERL single junction silicon solar cells are reported by researchers to have high efficiency (~ 20-25 %) and are promising for further improvement. Optimization is based on process and device simulation in SILVACO software package and integrating a Response Surface Methodology for optimal solution. Optimization of texture dimensions and ARC is followed by process parameters optimization for the emitter and base for best performance solar cell. A solar cell of efficiency 24 % is demonstrated by the simulation.

Keywords: *TEXTURE, ARC, DOPING PROFILE, HIGH EFFICIENCY SILICON SOLAR CELL, PERL, OPTIMIZATION.*

(Received 04 February 2011, in final form 01 December 2011)

1. INTRODUCTION

The energy conversion efficiency of silicon solar cells are increasing greatly due to the efforts of photovoltaic researchers throughout the world. The Passivated Emitter Solar Cell Structures PERL (Passivated Emitter Rear Locally Diffused) and PERT (Passivated Emitter Rear Totally Diffused), schematics shown in Fig. 1, are reported to have high energy conversion efficiency. Zhao et al. reported an efficiency of 24.0% [1], 24.7% [2] with PERL structure and 20.8% [4], 21.1% [3], 21.9% [3], 22.7% [4], 24.5% [2] with PERT structure. Benick et al. reported an efficiency of 23.2% [5] with PERL structure.

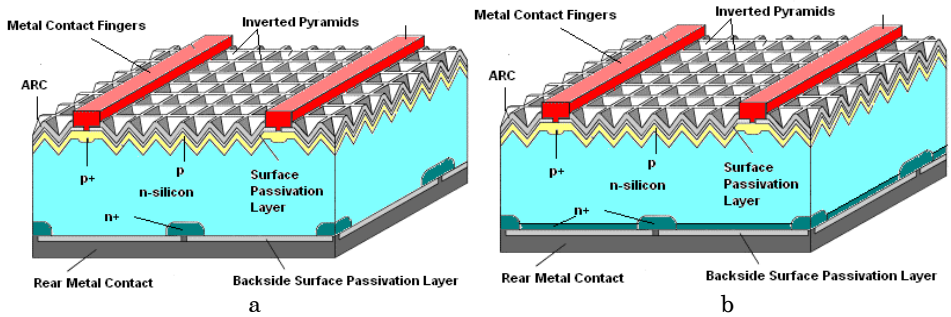

Fig. 1 *– PERL (a) and PERT (b) Solar Cell Structures (Adapted from Zhao et al. [1, 3])*

In order to explore the possibility of further improvement of efficiency in such structures a detailed simulation study is required. PC1D program is widely used for simulating crystalline silicon solar cells [6]. The simulation studies in this paper are carried out in SILVACO 2D (3D also possible) which has the capability to simulate both process and device simulations in one go. Such physically based simulation is needed in order to study the effect of various structure and process parameters in device performance. The physical structure of the solar cell used in our present study are designed using ATHENA module considering the standard silicon integrated chip processing technology and the electrical and optical characteristics are simulated using ATLAS module. The ATLAS device simulator module includes a wide variety semiconductor physics models for drift-diffusion transport, energy balance, quantum effect, SRH recombination, radiative recombination, Auger recombination, surface recombination, lattice heating, ray tracing, carrier generation, wide range of materials, Fermi–Dirac and Boltzmann statistics, doping effects, trap dynamics, band gap narrowing, tunneling etc. By using Silvaco Package a set of simulations were done to optimize texture and anti reflection coating followed by tuning of doping profile for increased efficiency.

2. SIMULATION AND OPTIMIZATION OF TEXTURE AND ANTI REFLECTION COATING

2.1 Structure

In order to achieve higher efficiency more photons should be absorbed in the given area for which texturing is done in solar cell structure. But, the effect of texturing, combining both optical as well as electrical behavior is to be studied, as increase in optical absorption in the cost of decrease in electrical collection efficiency due to structure change, would not help to increase the overall efficiency. In order to study the optical absorption behavior, a 250 μm thick ⟨100⟩ wafer structure was taken for simulation. Texture consisting of inverted pyramids of various base size (6-45 μm) were realized by etching and an ARC of 100 nm silicon nitride is deposited on the top of it. Fig. 2a shows the cross section of the structure considered for simulation depicting the ray tracing by the LUMINOUS module of the ATLAS. Fig. 2b shows the available photocurrent inside the structure without texturing, with texturing (7.5 μm base width) and with ARC for wavelength ranges between 0.3 μm to 1 μm.

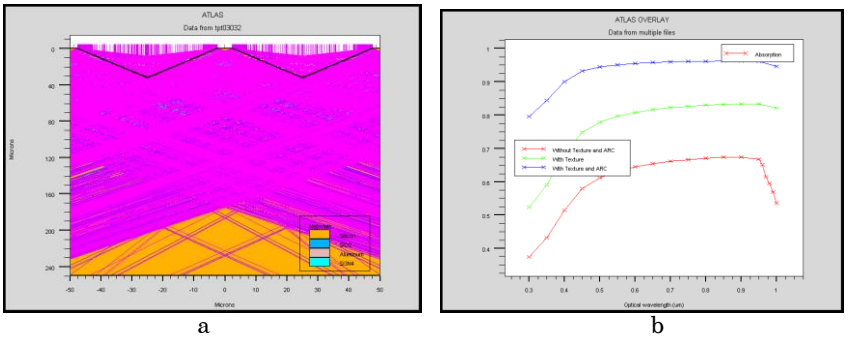

a b

Fig. 2 *– Cross section of textured structure showing ray traces spectral response showing effect of texture* (a) *and ARC* (b)

This depicts the ability of the considered models to include the effect of texturing and ARC in the structure.

2.2 Optimization of Texture Structure

Surface texturing increases the chance of reflected light to bounce back to the silicon surface itself and increases the effective surface area, thereby minimizing the reflection of photons to the surrounding air. If the base size of the inverted pyramid texturing is increased, then the effective surface area increases, which in turn increases absorption in the silicon structure. This is depicted in our simulation also as shown in the Fig. 3 for three different base sizes 7.5 μm, 20 μm and 45 μm without ARC. If bigger textures (> 10 μm) are made with lithography, the optical absorption efficiency can be increased. Using conventional chemical texturing the maximum achieved base size of pyramid is around 9 μm. So, texturing patterns has to be defined via photolithography. Though this lithographically defined texturing process is adding an additional processing step, this has another advantage as described in the next section.

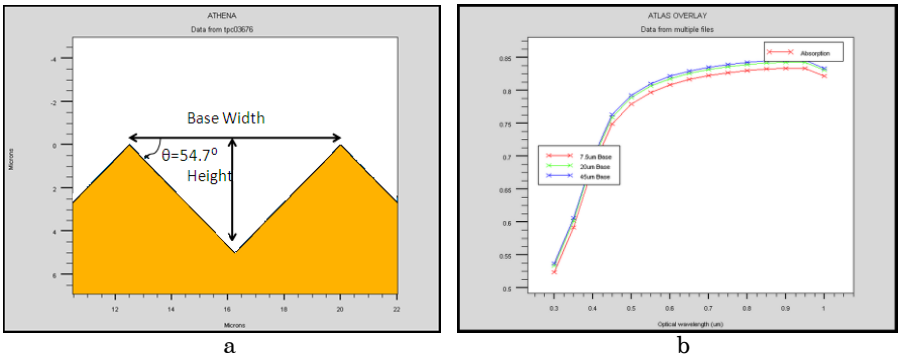

a b

Fig. 3 *– Pyramid dimensions (a) effect of change in texture dimensions without ARC (b)*

2.3 Optimum placement of Contacts

Now the issue comes where the contact can be kept in the textured solar cell surface. Conventionally, the contacts are kept as shown in the Fig. 4a and Fig. 1, one contact strip coming on the top of a hill among many hills of the cross section. The problem with such structure is that the carriers generated in other hills should pass through greater physical length in order to reach the contact. But in one contact strip per hill structure Fig. 4b the carriers can be collected efficiently within the hill. To study this effect a device simulation was done for same process steps, rear local diffusion of phosphorus at 840 °C for 30 min, front surface diffusion of boron for 60 min at 925 °C, front surface drive-in at 1050°C for 90 min with phosphorus base concentration of 1×10^{17}. But contacts were placed differently one having 10 μm contact placed between two inverted pyramids and the second with 5μm contact placed on the top of each hill, so that the shadowing effect is same and optical texturing is similar, Fig. 4a,b. From the comparison of this two it is found that the one contact per hill is giving higher efficiency than the former one as shown in Fig. 4c with 2.5 mA higher current density. Another advantage is that the same mask can be used for texturing, front surface selective emitter if needed and contact definition where instead of fingers, grid with square spacing will be used for making inverted pyramids.

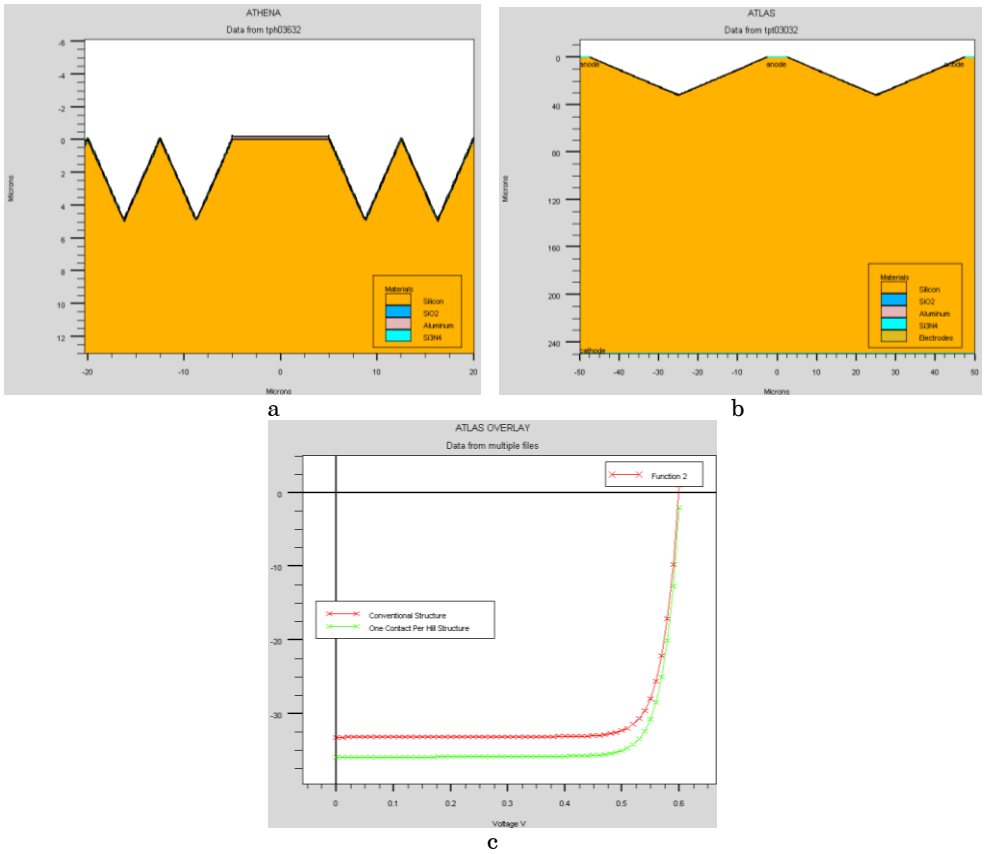

Fig. 4 *– Conventional PERL contact structure (a), one contact per hill (b) and Effect of one contact per hill (c)*

2.4 Dual Layer ARC

Already in Fig. 2b the effect of silicon nitride single layer ARC of thickness 100nm is depicted. Since Benick et al. [7] has used Al_2O_3-SiN_x for field effect passivation for n-type PERT solar cells, a simulation with dual layer ARC is done in order to optimize it and it was found that 10 nm Al_2O_3 (Refractive Index 1.72-1.84) and 60 nm SiN_x (2.0) is optimal as shown in Fig. 5 than 30 nm Al_2O_3 and 100 nm SiN_x ARC. This Al_2O_3 is responsible for very good surface field emitted passivation leading to very high carrier lifetime due to high negative interface charge (10^{13}) thereby within ARC we are getting good surface passivation also [10].

3. SIMULATION AND OPTIMIZATION OF DOPING PROFILE

3.1 Simulation Process

Optimization of optical absorption enhances the photogeneration of carriers, which should be efficiently collected before recombination. Hence the collection probability should be increased by optimizing the doping profile.

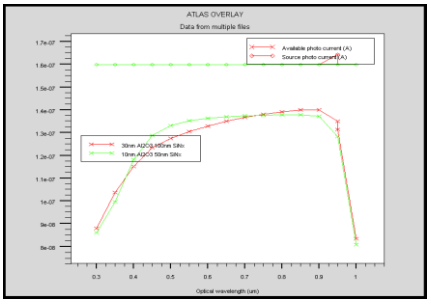

Fig. 5 *– Spectral response of Dual layer (Al_2O_3-SiN_x) ARC structure*

Efficient collection depends upon several process parameters like substrate doping concentration, front surface diffusion temperature and time; drive in tempera-ture and time; back surface diffusion temperature and time; surface passi-vation, thickness of the wafer, process sequence, and minority carrier lifetime. Since lots of variables are involved, the desirability method of Response Surface Methodology [11] is used in order to optimize the parameter towards best performance and this work has been carried out in SYSTAT 12.02 [9].

3.2 Efficiency Vs Substrate Concentration

The process and device simulation steps are shown as flowchart in Fig. 6. At first, ⟨100⟩ orientation, n-type 250 µm thick wafers, were considered for process and device simulation in which the substrate phosphorus doping concentration were changed from $1\times10^{14}/cm^3$ to $1\times10^{18}/cm^3$ range. Process steps were carried out in the same order as done by Jhao et al. [1]. Some of the assumptions taken in these simulations are the interface charge density of front surface passivating Al_2O_3-Si interface as $1\times10^{13}/cm^3$ [10] and back surface passivating SiO_2-Si interface as $1\times10^{10}/cm^3$. After defining selective mask on backside with 5µm window where contact will be taken, a rear local diffusion of phosphorus was done at 840 °C for 30 min. Then lithographically defined textures were defined on the front side for one contact per hill structure. This was followed by a front surface diffusion of boron for 60 min at 925 °C. Then a drive-in was done at 1050 °C for 60 min followed by top and bottom passivation and contact definition. Then the structure was illuminated by AM 1.5 Spectrum and the IV characteristics was obtained. Fig. 7a illustrates the doping profile of the structure taken for simulation at two cutlines showing a junction depth of 1 µm in both front and back.

The power conversion efficiencies for the above processing steps for different wafer concentrations are shown in Fig. 7b. The power conversion efficiency started with a low value of 14.04 % at $1\times10^{14}/cm^3$ substrate concentration and reached a maximum of 19.36 % for $1.5\times10^{16}/cm^3$ and then dropped to 10 % at $1\times10^{18}/cm^3$ concentration. This is because for higher efficiency, minority carrier concentration should be lower so that recombination rate is lower. For this the doping concentration corresponding to majority carriers should be kept higher. But, in other hand diffusion length should be higher for higher efficiency and this diffusion length decreases with increased doping. Therefore doping concentration should be kept lower which results in a tradeoff between diffusion length vs recombination rate. Therefore an optimal

value of substrate doping concentration is needed which was found from simulation to be closer to $1.5\times10^{16}/cm^3$ (3 Ohm·cm) for the above processing steps where efficiency reaches the maximum.

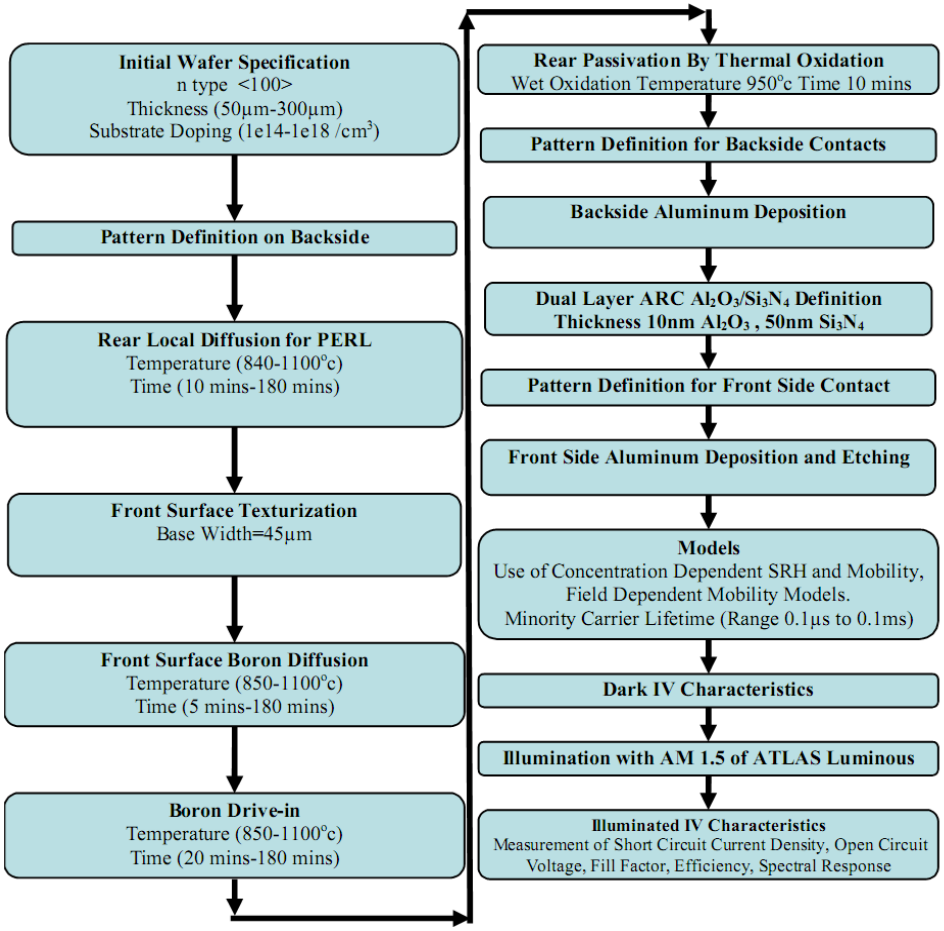

Fig. 6 *– Process design flow for solar cell simulation*

3.3 Effect of Front Surface Diffusion and Drive-in Parameters

The above processing steps were repeated by keeping substrate concentration as $1.5\times10^{16}/cm^3$ and front surface drive-in temperature was varied from 850 to 1200 °C keeping time as constant 60 min and front surface drive-in time was varied from 20 min to 180 min keeping temperature as 1200 °C. The solid solubilities of corresponding temperatures were given as input along with time and temperature. Fig. 8a shows the surface plot of the response obtained which indicates that significant increase is there only for drive-in at temperature greater than 1050 and time greater than 90 min creating deeper junctions. But very much higher temperature and time would increase the thermal budget. So further simulations were done to search other optimal parameters so that this high temperature processes can be avoided.

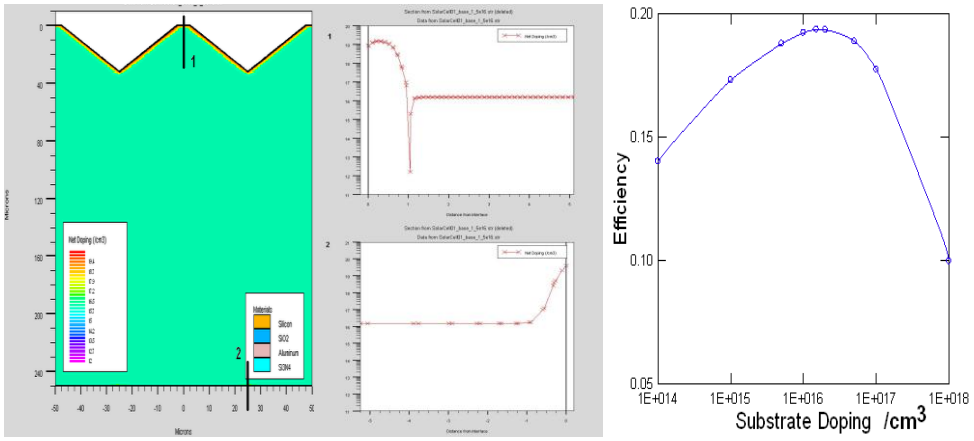

a *b*

Fig. 7 *– Doping profile of Front Surface Diffusion/Rear Local Diffusion (a) Efficiency Vs Substrate Doping (b)*

Now the processing steps are carried out by keeping drive in temperature as 1200 °C, time as 120 min and a series of simulations were done by varying Front Surface Boron Diffusion time from 5 min to 180 min with diffusion temperature as 925 °C. Similarly another series of simulations were done by keeping diffusion time as 5 min and temperature varied between 850 to 1100 °C. The results are shown in Fig. 8b in which the variation with respect to temperature resembles that of Efficiency Vs. Substrate Concentration Fig. 7b as expected due to carrier diffusion length-minority carrier lifetime tradeoff and hence the optimal values of boron diffusion temperature is 850 to 950 °C. There is a small increase in efficiency as the diffusion time is decreased and hence a diffusion time of greater than 5 min and less than 20 min is sufficient.

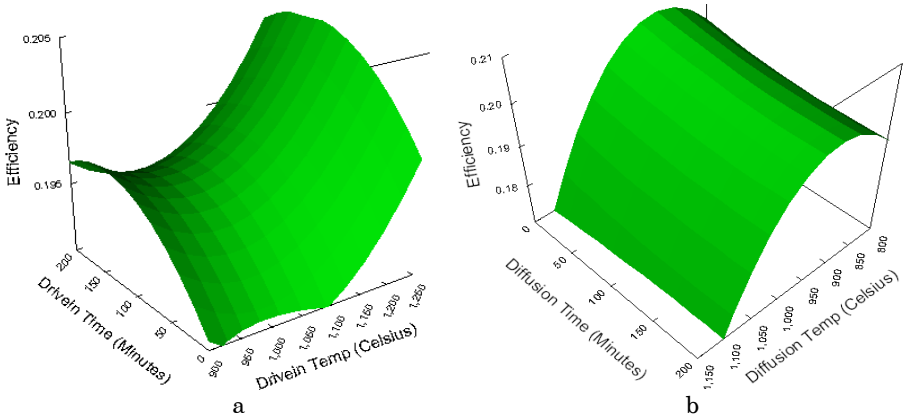

a b

Fig. 8 *– Response Surface plot of Front Surface Drive-in (a)Front Surface Diffusion (b)*

3.4 Effect of Rear Local Diffusion Parameters

The rear local diffusion is to keep away holes away from the contact so that recombination won't happen there. The above processing steps were repeated with temperature being varied from 850 to 1200 °C keeping time as constant 60 min and the same way diffusion time was varied from 10 min to 180 min keeping temperature as constant 840 °C. But there is no significant changes in the efficiency as observed in Fig. 9. An absence of Rear Local Diffusion brought the efficiency down to 18.64 %.

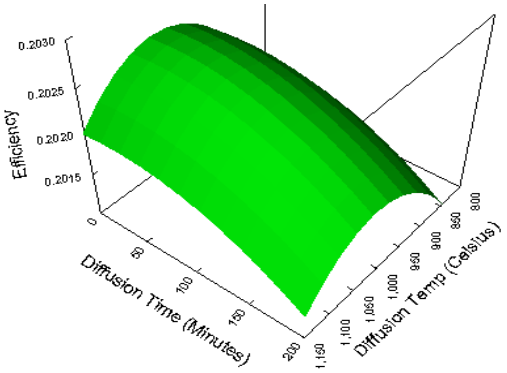

Fig. 9 *– Response Surface plot of Rear Local Diffusion Parameters*

3.5 Effect of Thickness of Wafer

The thickness of the wafer was varied from 50 µm to 300 µm with all other parameters kept as optimized above. The efficiency increased gradually as the wafer thickness was decreased and at 50 µm it gave an efficiency of 22%. As the main transport mechanism in such a structure is diffusion, lesser thickness is resulting in higher efficiency since the carriers can diffuse to their respective contacts sooner since it can diffusion current will be higher. But we cannot go for such thin wafers as it is prone to breakage.

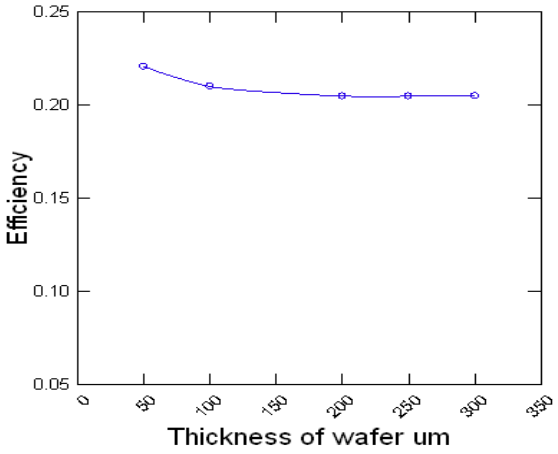

Fig. 10 *– Effect of thickness of Wafer*

3.6 Effect of Carrier Lifetime

A total of 78 simulations were done based on successive outputs from desirability plots of Response Surface Methodology. Based on that for further simulation was done as follows with considerably low thermal budget. Rear local diffusion of phosphorus was done at 840 °C for 30 min. Front surface diffusion of boron was done for 10 min at 900 °C. Front surface drive-in was done at 1050 °C for 90 min. Then the J-V Characteristics for different lifetime from 0.1 µs to 0.1 ms for the above parameters were obtained. It is shown in Fig. 10 and the various output parameters corresponding to different lifetimes are shown in the table 1. An efficiency of 24.01 % is shown in it for a SRH lifetime of 100 µs. Practically the SRH lifetime has even reached a few ms in case of high quality Passivated wafer which in turn would increase the efficiency further [10].

Table 1 *–Simulated Output Parameters of the processed solar cell*

S. No	SRH Lifetime µs	J_{sc} mA/cm^2	V_{oc} V	Fill Factor	Efficiency %
1	0.1	28.4	0.5196	0.785	11.64
2	1	38.2	0.5655	0.8157	17.62
3	10	42.1	0.6034	0.83	21.04
4	100	44.4	0.6464	0.8366	24.01

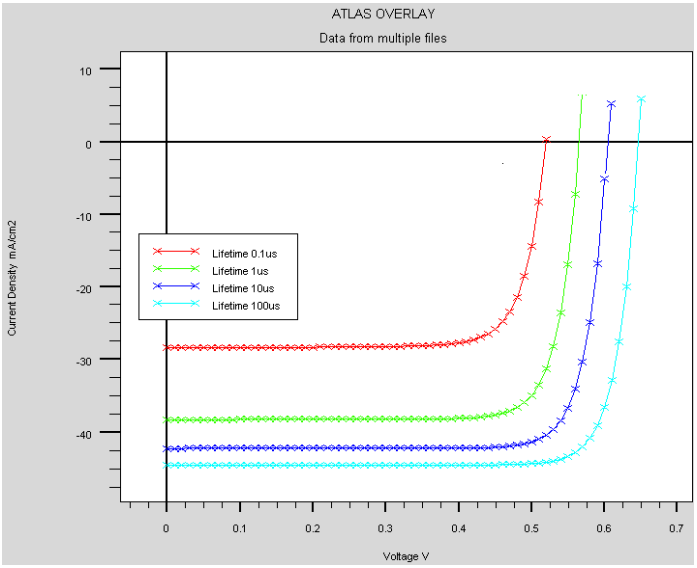

Fig. 10 *– IV Characteristics for different lifetimes*

4. CONCLUSION

Thus, simulation and optimization of PERL silicon solar cell structure is done integrating response surface methodology with Silvaco. The simulation indicates that one contact per hill structure can give better output than

conventional PERL contact structure. Based on the response surface plots it is clear that for higher efficiency, substrate concentration, front surface diffusion and drive-in are key parameters to consider in addition to good surface passivation and higher wafer quality for lifetime enhancements. Fabrication with substrate concentrations of range 1.5×10^{16} to 5×10^{16}, front surface diffusion temperature of 850 to 950 °C, and a drive-in at temperature 1050 °C for 90 min, with good passivation are expected to give efficiency about 20 %. Efficiency of 24 % is demonstrated by simulation for 100 μs SRH lifetime. The simulations reveal PERL structures as an attractive scheme for high efficient solar cells.

The authors would like to thank Dr. Chandrasekhar, Director, CEERI for his motivation and Dr. C. Dhanvantri, Head, ODG, CEERI for giving access to Silvaco package.

REFERENCES

1. J. Zhao, A. Wang, P.P. Altermatt, S.R. Wenhama, M.A. Green, *Sol. Energ. Mat. Sol. C.* **41-42**, 87 (1996).
2. J. Zhao, A. Wang, P.P. Altermatt, S.R. Wenhama, M.A. Green, *Sol. Energ. Mat. Sol. C.* **65**, 429 (2001).
3. J. Zhao, A. Wang, *4th World Conference on Photovoltaic Energy Conversion, Waikoloa,* USA, 996 (2006).
4. P. Engelhart, N.P. Harder, R. Grischke, A. Merkle, R. Meyer, R. Brendel, *Prog. Photovolt. Res. Appl.* **15**, 237 (2006).
5. D.A. Clugston, P.A. Basore, *26 IEEE Photovoltaic Specialists Conference*, 207 (1997).
6. J. Benick, B. Hoex, M.C.M. van de Sanden, W.M.M. Kessels, O. Schultz, S.W. Glunz, *Appl. Phys. Lett.* **92**, 253504 (2008).
7. *Athena User's Manual* (Silvaco International), (2004).
8. *Atlas User's Manual* (Silvaco International), (2004).
9. *Systat V12.0 Help Contents*.
10. B. Hoex, J. Schmidt, R. Bock, P.P. Altermatt, M.C.M. van de Sanden, W.M.M. Kessels, *Appl. Phys. Lett.* **91**, 112107 (2007).
11. S. Raissi, R.-E. Farsani, *World Academy of Science, Engineering and Technology*, **51** (2009).